Linearization of modal parameters in Duffing oscillator using the random decrement technique

K. K. Vesterholm [1,*], **R. Brincker** [2] , **A. Brandt** [1]
[1] University of Southern Demark, Department of Technology and Innovation
Campusvej 55, DK-5230 Odense M, Denmark
[*] Corresponding author e-mail: **kav@iti.sdu.dk**

[2] Technical University of Denmark, Danish Hydrocarbon Research and Technology Centre
Anker Engelunds Vej 1, DK-2800 Kgs. Lyngby, Denmark

Abstract
In this study, it is investigated how the random decrement (RD) technique can be used to linearize the nonlinear stiffness of a single degree of freedom system with a hardening spring, known as a Duffing oscillator. The linearization is implemented by using a set of trigger levels in the response signal to define RD signatures. The modal parameters are estimated at the same response level for various excitation force levels, from the RD signatures describing the system at that specific level, and extracting the modal parameters using time domain parameter extraction methods. The system described by the RD signature is assumed to behave as a linear system with an equivalent stiffness depending on the trigger level. Various triggering conditions for the RD technique are investigated, to study their applicability in linearizing the nonlinear system. The results of the study show that, with the Local Extremum, and Envelope triggering condition, the RD technique can be successfully used to linearize the modal parameters of the Duffing oscillator.

1 Introduction

The random decrement (RD) technique is an established method for evaluating modal parameters of structures under random force inputs. Since the RD technique can be applied at a specific response level, it is an obvious step to apply it on multiple levels in the same signal, to investigate the response for amplitude dependent nonlinearities. Using this approach, it should be possible to examine if, and how the modal parameters vary at different response amplitudes, and thereby linearizing the nonlinearity. The idea of analyzing systems with amplitude dependent nonlinearities has been part of the RD technique since H. A. Cole introduced it in 1968 [1], where he showed that the technique is promising regarding the detection of amplitude dependent nonlinearities. The results from this study can be used in any application where a nonlinear dynamic system is excited by a random force, and the amplitude dependent properties need to be identified.

S. R. Ibrahim et. al. introduced multi-triggering in 1987 [2] to identify amplitude dependent nonlinearities, and investigated various triggering conditions including the level crossing (LC) condition. The modal parameters were identified with the Ibrahim Time Domain (ITD) method. In 1992 A. P. Jeary [3] also used multiple triggering levels with the LC triggering condition and suggested that a nonlinearity in the natural frequency can appear as a decay function. A new triggering condition was proposed in 1996 by Tamura and Suganuma [4], which in the present paper is referred to as local extremum (LE), to identify amplitude dependent nonlinearities. A numerical study was performed, where the system parameters were simulated to be dependent on the previous peak in the response, and constant between peaks. The RD technique with LE was then applied to a wind-induced response of various buildings. The amplitude envelope RD technique

was introduced in 2016 by Huang and Gu [5]. RD was used here under the assumption that the dynamic parameters of the system do not change within the individual signal segments, and that the system parameters, corresponding to the triggering level, is contained within the corresponding segment. The numerical study in [5] introduces a new iterative computing method that uses the Newmark method, and the system is modelled such that the stiffness and damping are functions of the amplitude envelope of the response. A review of various implementations of the RD technique was performed in 2017 by T. Reynolds [6], who compares the level crossing, local extremum, envelope, and positive point (see Section 2.2). The review was done by performing a Monte-Carlo simulation with the computation method introduced in [5] with amplitude dependent damping in an SDOF system. The review concludes that local extremum, envelope, and positive point give good estimates of the nonlinear parameters compared to level crossing, but have higher variability.

In the present paper we study the duffing oscillator, which has a nonlinear restoring force, see Figure 1. It is investigated how accurately the RD technique can identify the linear and nonlinear parts of the restoring force, by testing various triggering conditions.

In a linear system, the modal parameters are the same, regardless of the level of excitation force, because the principle of superposition is valid. For a nonlinear system, like the Duffing oscillator, the principle of superposition no longer applies, and modal parameters are dependent on the level of excitation force. For the linearization of modal parameters to be successful, investigating a specific response level of the system being excited by one level of force, should reveal the same modal parameters when investigating the same specific response level, where the system is excited by another level of force. I.e. the linearization of the system should only be dependent on the system parameters and not the excitation force.

In the present work, several numerical examples are analyzed with various triggering conditions. From the RD signatures, modal parameters are extracted and the natural frequencies are then used to calculate the linearized restoring force.

2 Theory

In this section the theory for the linearization of the Duffing oscillator, and the RD technique is described.

2.1 Duffing oscillator

The Duffing oscillator is described by Duffing's equation [7]

$$m\ddot{x}(t) + c\dot{x}(t) + kx(t) + k_3x^3(t) = F(t) \tag{1}$$

where m, c and k are the linear mass, damping, and stiffness respectively, k_3 is the nonlinear stiffness, x is displacement, and F is the applied force. The Duffing oscillator can be described as a single degree of freedom (SDOF) system, with a cubic spring attached, see Figure 1. When the nonlinear stiffness k_3 is positive it is interpreted as a hardening spring.

The nonlinear part of Equation (1) is included in the total restoring force

$$F_{rest}(t) = kx(t) + k_3x^3(t). \tag{2}$$

It is assumed that the total restoring force can be reformulated as

$$F^*_{rest}(\alpha, t) = k^*(\alpha) \cdot x(t) \tag{3}$$

where the equivalent stiffness k^* is dependent on some amplitude α. This assumption results in a linearized form of Duffing's equation

$$m\ddot{x}(t) + c\dot{x}(t) + k^*(\alpha)x(t) = F(t), \tag{4}$$

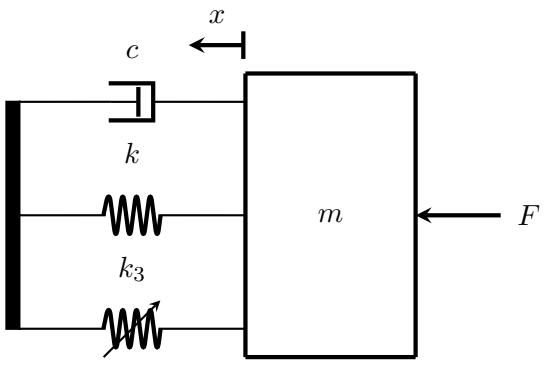

Figure 1: Single degree of freedom system with cubic spring, also called Duffing oscillator

where the system is interpreted as being linear for a specific amplitude α.

With the introduction of an amplitude dependent stiffness, the relative damping also changes with amplitude. The amplitude dependent relative damping is described by [8]

$$\zeta(\alpha) = \frac{c}{2\sqrt{mk^*(\alpha)}} \tag{5}$$

which means ζ will decrease when k^* increases.

2.2 Random Decrement

This section will explain how the RD technique is performed, and specify the triggering conditions used in the present study.

The RD technique is the method of obtaining the RD signature, which is calculated as an average of N signal segments extracted from $x(t)$ [9]

$$\hat{D}_{X,Y}(\tau) = \frac{1}{N}\sum_{i=1}^{N} x(t_i + \tau)|T_{y(t_i)} \tag{6}$$

where x and y are realizations of the stochastic processes X and Y. N is the number of time points in process y that satisfies the triggering condition $T_{y(t_i)}$ at the time points t_i. τ is the lag of the RD signature, which extends from $-M$ to M. In Figure 2, the algorithm to perform this calculation is illustrated, where the level crossing (LC) triggering condition is used. The algorithm is explained stepwise by following the steps 1 - 4:

1) The triggering condition LC is applied to signal $y(t)$ to find the time point t_i. Four triggering points are found, which are marked by dots.

2) The triggering points t_i, found in signal $y(t)$ are transferred to $x(t)$ to mark the centers of the segments, that are extracted from the signal $x(t)$. The segments are symmetrical around the triggering points.

3) The four individual segments, extracted from signal $x(t)$, are illustrated on top of each other in the lag domain.

4) The average of the four segments results in the RD signature. Since only four segments are extracted the RD signature is not complete and it has a large random error, but the general outline is quite clear.

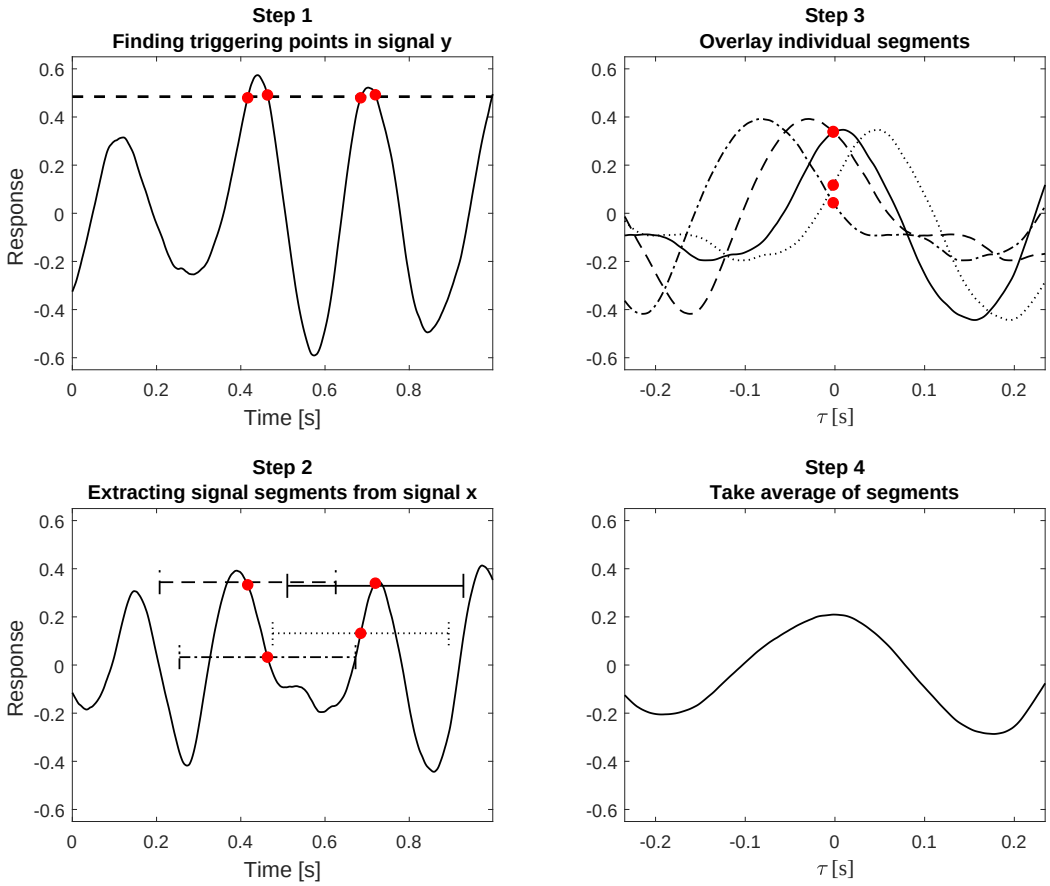

Figure 2: By following steps 1-4, it is illustrated of how the random decrement technique is performed, according to Equation (6). Here, the level crossing triggering condition is applied

There are two forms of RD signatures. Auto RD signature $\hat{D}_{X,X}(\tau)$, where both the triggering condition is applied to, and the segments extracted from, signal $x(t)$. Cross RD signature $\hat{D}_{X,Y}(\tau)$, where the triggering condition is applied to signal $y(t)$ and the segments are extracted from signal $x(t)$, as shown in Equation (6) and illustrated in Figure 2.

There are many triggering conditions, and this study will be investigating how four of them perform when analyzing the Duffing oscillator, namely level crossing (LC), positive point (PP), local extremum (LE), and envelope (ENV). There is a confusion in the naming of triggering conditions, and for consistency the triggering conditions PP, LE, and LC are named to correspond with [9]. This study presents a modified version of the envelope triggering condition presented in [5].

The LC triggering condition is the one H. A. Cole used when he introduced the RD technique [1]. The condition states, that a triggering point is detected if the signal is equal to a triggering level a

$$T^{LC}_{y(t)} = \{y(t) = a\}. \tag{7}$$

In the PP triggering condition, a triggering point is detected when the signal is between two triggering bounds a_1 and a_2

$$T^{PP}_{y(t)} = \{a_1 \leq y(t) < a_2\}. \tag{8}$$

For LE a triggering point is detected when the signal satisfies two conditions. It has to be between the two triggering bounds, a_1 and a_2, and the derivative of the signal has to be equal to zero, which is equivalent to

a local maximum or minimum

$$T_{y(t)}^{LE} = \{a_1 \leq y(t) < a_2, \dot{y}(t) = 0\}. \tag{9}$$

The ENV triggering condition uses the same principle as PP, but instead of using signal $y(t)$ to find the triggering points, the amplitude envelope of $y(t)$ is used. The amplitude envelope is calculated as the magnitude of the analytical signal

$$A(t) = |y(t) + j\tilde{y}(t)| \tag{10}$$

where $\tilde{y}(t)$ is the Hilbert transform of $y(t)$ [11]. The triggering condition is defined as

$$T_{y(t)}^{ENV} = \{a_1 \leq A(t) < a_2\}. \tag{11}$$

ENV is not as well understood as the other triggering conditions, and exactly how it works leaves room for discussion in another study. An interpretation of ENV could be that the amplitude envelope $A(t)$ represents equivalent peaks in the signal, and using it to find triggering points is equivalent to LE. The difference is that the triggering points found are not restricted to a response with zero slope, that is the case for LE, but the extracted segments have the same properties. With the triggering condition ENV, the identified triggering points are not located neatly around the triggering level, as is the case for the other triggering conditions, but spread out in both the positive and negative part of the response.

In [10] it is shown that the RD signature is proportional to the correlation function in the following way

$$D_{X,Y} = \frac{R_{X,Y}(\tau)}{\sigma_X^2} \cdot \tilde{a} - \frac{\dot{R}_{X,Y}}{\sigma_{\dot{X}}^2} \cdot \tilde{b} \tag{12}$$

where σ^2 is the variance and $\tilde{a}$ is a function of the triggering bound and the signals' probability density function, and is related to the part of $T_{y(t)}$ that is applied to the response. $\tilde{b}$ is a function of the triggering bound and the signals' probability density function, and is related to the part of $T_{y(t)}$ that is applied to the derivative of the response[9].

One of the assumptions for the RD technique is that a response signal can be decomposed into three parts; the response due to initial displacement, the response due to initial velocity, and response due to the excitation force. When averaging the segments, the excitation force averages out, since it is assumed to have zero mean. The velocity part is removed by making sure that if a triggering point is on a positive slope, another triggering point is on the negative part of a slope, so they cancel out, and in most cases this is what happens around a peak with PP and LC, as can be seen in Figure 2. Another way to eliminate the velocity part is by only triggering on samples that have no velocity, which is the principle for LE.

For this study, the RD technique is applied, by first identifying the triggering points in the positive part of the response, calculating the RD signature from the extracted segments, then identifying the triggering points in the negative part of the response by multiplying the triggering level with -1, calculating the RD signature from these extracted segments as well. The RD signature from the negative part of the response is multiplied by -1, and an average is taken of the RD signatures from the positive and negative parts of the response. The final step is to flip the part of the RD signature with negative lags over to the positive side, and again taking an average of the two. The RD signature is now finalized and ready for the next step in the analysis.

3 Numerical tests and analyses

The numerical tests are performed by simulating the forced response of mechanical systems in the time domain using a digital filter based method [12], and is done with a sampling frequency of $f_s = 1024$ Hz. The excitation force is a normal distributed signal with different variances, representing various force levels. The force is low pass filtered at 100 Hz with a 4th order Butterworth filter before exciting the system. All time history responses are 81.2 minutes resulting in 4990000 samples, and no noise is added in the

System	Mass	Damping	Linear Stiffness	Nonlinear Stiffness
#	[kg]	$[\mathrm{Nsm}^{-1}]$	$[\mathrm{Nm}^{-1}]$	$[\mathrm{Nm}^{-3}]$
1	0.50	0.4	1000	0
2	0.50	0.4	1000	500
3	0.50	0.4	1000	2000
4	0.50	0.4	1000	4000

System	Mass	Damping	Linear Stiffness	Nonlinear Stiffness
#	[kg]	$[\mathrm{Nsm}^{-1}]$	$[\mathrm{Nm}^{-1}]$	$[\mathrm{Nm}^{-3}]$
5	0.65	0.8	1500	0
6	0.65	0.8	1500	750
7	0.65	0.8	1500	1500
8	0.65	0.8	1500	3500

System	Mass	Damping	Linear Stiffness	Nonlinear Stiffness
#	[kg]	$[\mathrm{Nsm}^{-1}]$	$[\mathrm{Nm}^{-1}]$	$[\mathrm{Nm}^{-3}]$
9	350	400	1.5e6	0
10	350	400	1.5e6	1.7e15
11	350	400	1.5e6	1.7e14

Table 1: Mechanical systems that are investigated

simulations. In the present study, the simulated response is a displacement signal. Several mechanical systems are investigated to conduct a thorough analysis, and are presented in Table 1. Each system is excited by 11 different force levels.

After the responses have been simulated the next step is to set up the RD analysis.

In [9], it is recommended that the triggering level should not be below the standard deviation of the response signal σ_y, and not above $2\sigma_y$. This recommendation is made on the basis of an analysis of linear systems. The triggering levels in the present study is chosen with two things in consideration; the recommendation from [9], and a desire to investigate a large range in the response signal. These considerations results in triggering levels in the interval $[\sigma_y, 2.5\sigma_y]$ for the present analysis.

The triggering levels are defined for each system as 75 logarithmically spaced levels, where the lowest triggering level is the standard deviation of the response for the case where the system is excited by the lowest force level, and the highest triggering level is 2.5 times the standard deviation of the response when the system is excited by the highest force level. When the system is then analyzed, the response can be divided to approximately 16 levels in the interval $[\sigma_y, 2.5\sigma_y]$ for each case with a different force level. This allows for an easy comparison between cases of different force levels, because the triggering levels are at the same specific response levels.

For the triggering conditions PP, LE, and ENV, where two levels are needed to define a triggering point, the levels $[a_1, a_2]$ form a triggering band. When using a triggering band, and analyzing amplitude dependencies, there are a few things to consider. It is desired to calculate an accurate RD signature using Equation (6), meaning that N should be large, which can be realized by having a wide triggering band. However, the analysis is desired to reveal information about a specific amplitude, meaning that the band should be narrow, and thereby having a well defined amplitude. The triggering band is defined as a_2 being the level specified above, and a_1 is tweaked such that an amplitude is well defined, while also having a large N to calculate an accurate RD signature. For PP a_1 is chosen to find approximately 10000 triggering points in the response signal, and for LE, there are found approximately 3500 triggering points. For ENV the band is in the amplitude envelope $A(t)$, and a_2 is still as defined above, but a_1 is now defined such that the band $[a_1, a_2]$ represents 0.1% of the range of $A(t)$.

The number of lags in the RD signature must be defined through the number M, and for all analyses performed in the present study $M = 1024$. This is a very large M, and only the first 110 lags are involved in the further analysis, but this allows the analyst to visually inspect the RD signatures during the investigations, with a lot of information available.

With these settings, the RD analysis can be performed on all systems, and an example of RD signatures with three triggering levels, from a linear and a nonlinear system is presented in Figure 3. The case illustrated,

is for systems 1 and 3, both excited with an rms force of 89 N. It is very clear that for the linear system, only the scaling of the RD signature changes with triggering levels high, middle or low. The signatures from the nonlinear systems experience other changes as well as scaling of the RD signature, an indicator that this system is in fact amplitude dependent.

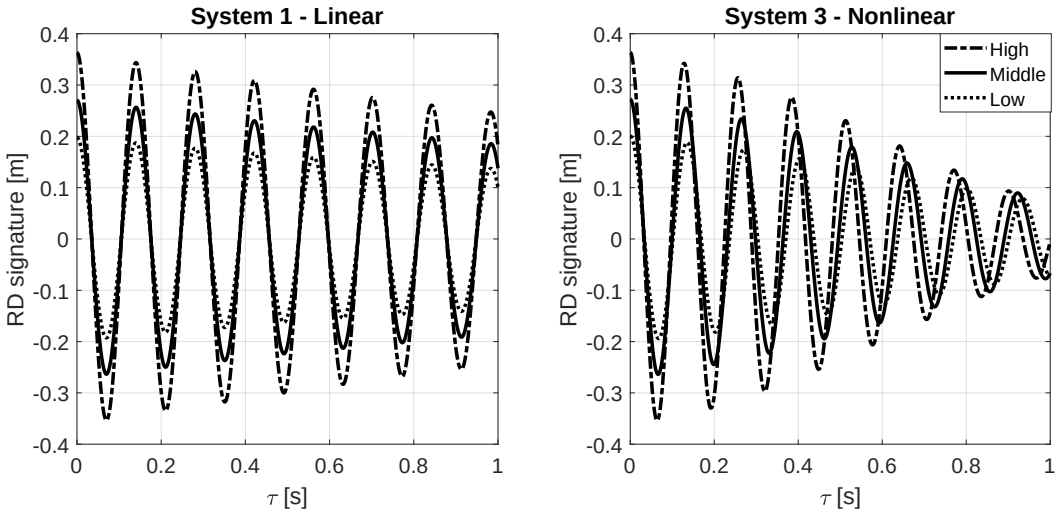

Figure 3: Comparison of 3 RD signatures from a linear an a nonlinear system. The systems 1, and 3, are both excited by a force with rms level of 89 N, and analyzed with the LE triggering condition

Once the RD signatures are obtained, they are treated as correlation functions, and the modal parameters are extracted using time domain methods. In the present study, three methods are compared, Prony [13], Least Squares Complex Exponential (LSCE) [14], and Ibrahim Time Domain (ITD) [15]. The modal parameter extraction methods are all applied using the ABRAVIBE toolbox [16], where the methods are implemented using stabilization diagrams. The first 10 lags are excluded from the RD signatures, and the following 100 lags are used in all the modal parameter extraction methods.

4 Results and Discussion

There are two main results presented and discussed in this section. First, results concerning the question whether it is possible to linearize the modal parameters independently of the excitation force level. And second, how accurately the nonlinearity is identified.

In the investigation, the deviations between the parameter estimation methods is minimal, and only results for Prony are presented.

The four different triggering conditions are compared, to evaluate whether they can be used to linearize the nonlinear systems independently of the excitation force level. The results presented here are from the analysis of system 4, as these are representing the general results from all the systems very well.

In Figure 4, the estimated frequencies are given as a function of triggering level for the four triggering conditions, each line in the plots represents a case of the system being excited by a specific rms force level. The different ranges in triggering levels for the different cases, stems from the fact that the variance of the response gets large when the system is excited by a larger force, and the triggering levels are logarithmically spaced in the interval $[\sigma_y, 2.5\sigma_y]$ for the individual case.

When comparing the four triggering conditions in Figure 4, it is easy to see that PP and LC behaves differently from LE and ENV. Focusing on the triggering level around 0.3 m, the 4 cases with the rms forces 66.9 N, 89.3 N, 112 N, and 134 N are represented. Triggering conditions PP and LC do not identify the same frequency for the four cases at this triggering level, instead the frequency increases with the applied force. If

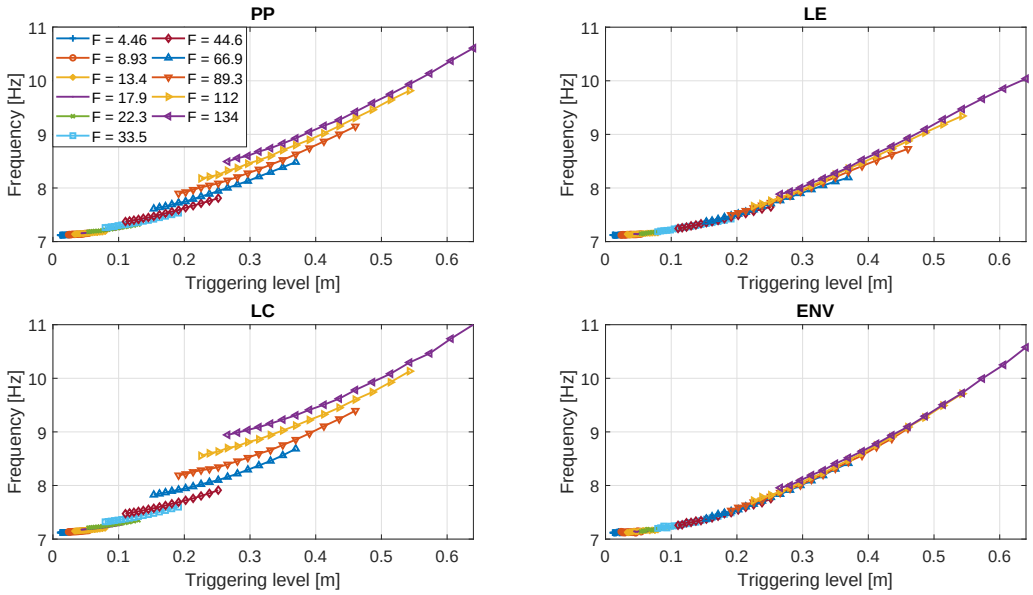

Figure 4: Example of estimated eigenfrequencies as a function of triggering level. The present analysis is done on system 4. The various curves represent cases with different rms force applied to the system

the curves in PP and LC, for the rms force of 134 N, would be described by a function, it would not be the same function that described the other curves. For LE and ENV, the frequency estimates are nearly the same for the various rms force levels, and a single function could describe all the curves, since they all overlap.

From this comparison, the triggering conditions PP and LC cannot linearize the eigenfrequencies independently of the excitation force, while LE and ENV can. This pattern repeats for all systems, and all modal parameter extraction methods.

The exact reason why PP and LC are not capable of the desired linearization is unknown. It is however known that it is not because PP and LC triggers on samples with a slope and LE does not, because ENV finds most triggering points on a slope.

According to Equation (5), the relative damping decreases as a function of triggering level. In Figure 5 the damping estimates are presented as a function of triggering level. As in Figure 4, each line in the plots represents a case of the system being excited by a specific rms force level. Again the triggering conditions PP and LC behave in a comparable way, while differing from LE and ENV. For rms force levels below 44.6 N, all triggering conditions result in an acceptable damping estimate, but PP and LC give an erroneous amplitude dependent damping estimate when the excitation force is increased. LE and ENV lead to acceptable damping estimates for a larger range of rms force levels. When the force exceeds 89.3 N, the estimates have a slight increasing trend, while the true relative damping is decreasing, resulting in up to 100 % difference between the true, and the estimated damping for the highest triggering levels. The damping estimates when using LE and ENV are quite poor, but the error is similar for the various force levels.

At the triggering level of 0.33 m, four cases with the rms forces 66.9 N, 89.3 N, 112 N, and 134 N, are represented. If the linearization is independent of the force level, it is expected that the RD signatures, from this triggering level, will have the same appearance. A comparison of the RD signatures at that triggering level is done in Figure 6, and here the trend continues, where the PP and LC look very similar, but differing from LE and ENV. It should be noted that LE and ENV also are very similar, except for the scaling. The RD signatures of LE and ENV for the different force levels are very similar in the first part, and as the lags increase, the RD signatures appear to be increasing slightly in frequency and damping, when the force level increases. For PP and LC, the increase in frequency and damping, as the force level increases, is significant, and the RD signatures do not appear to be describing the same system. These observations from the RD

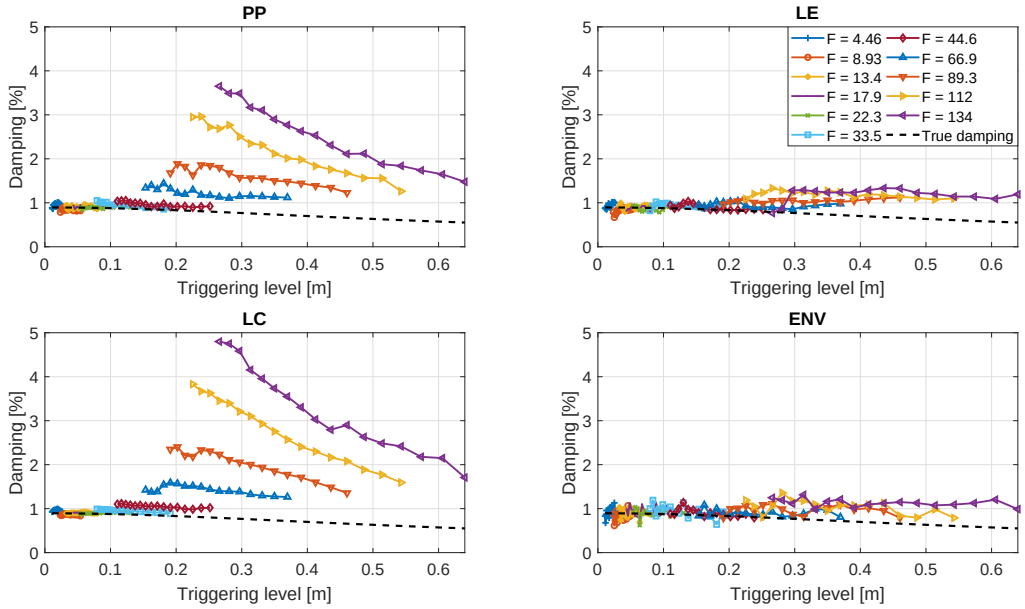

Figure 5: Example of estimated damping as a function of triggering level. The present analysis is done on system 4. The various curves represent cases with different rms force applied to the system. The true damping is calculated with Equation (5), using the triggering level as α

signatures are corresponding very well with the estimated eigenfrequencies and damping factors in Figures 4 and 5.

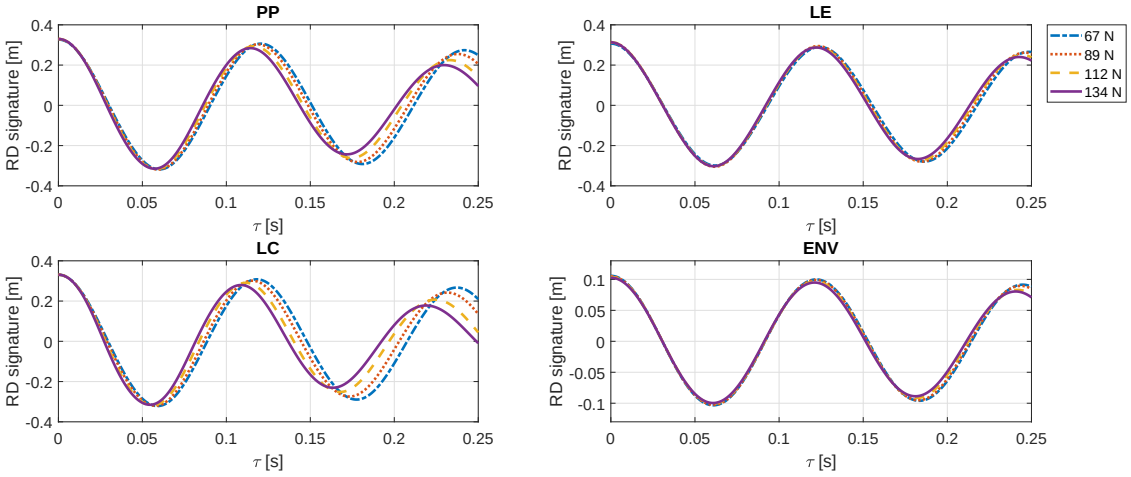

Figure 6: RD signatures for system 4, with four different levels of force, all at the triggering level 0.33 m

The accuracy, with which the nonlinearity is identified, is evaluated on the basis of how well Equation (3) can be fitted to Equation (2). This means that the equivalent stiffness must be calculated for each triggering level (Tl_i)

$$k^*(Tl_i) = m\left(2\pi f(Tl_i)\right)^2 \tag{13}$$

where $f(Tl_i)$ is the estimated eigenfrequency as a function of the triggering level as presented in Figure 4. With the equivalent stiffness, the equivalent restoring force is calculated, using the triggering levels as the displacement term

$$F^*_{rest}(Tl_i) = k^*(Tl_i) \cdot Tl_i. \tag{14}$$

This interpretation of the restoring force says that the system- and modal parameters are both extracted from, and describing the system, at that specific triggering level.

As mentioned above, PP and LC cannot linearize the eigenfrequency independently of the excitation force, and it does not make sense to describe the corresponding restoring force with a single function. Therefore, PP and LC are excluded for the next part of the discussion.

In order to evaluate how well the linearization describes the nonlinear restoring force, an average is taken of the restoring forces, calculated for the individual cases of various excitation force levels, producing a single curve with which to perform the fit. The RD signatures are calculated by applying the technique to both the positive and negative parts of the response, as mentioned in Section 2.2. Because the RD signatures are calculated from both the positive and negative parts of the response, both the negative and positive parts of the restoring force can be used in the fitting. A duplicate of the average restoring force is therefore rotated 180° representing the negative parts of the restoring force. A combination of the positive and negative parts, forms the antisymmetric curve that is the restoring force as a function of the triggering level, see Figure 7.

In Figure 7, the estimated restoring force of system 10 for both ENV and LE is compared with a reference restoring force, which is calculated with Equation (15) where the stiffness coefficients for the system, and the triggering level as the displacement term is inserted. Both ENV and LE fails to fit completely with the true restoring force of the system, as the cubic part of the function is underestimated in both cases. When focusing on the linear part, around zero, both ENV and LE fit very well.

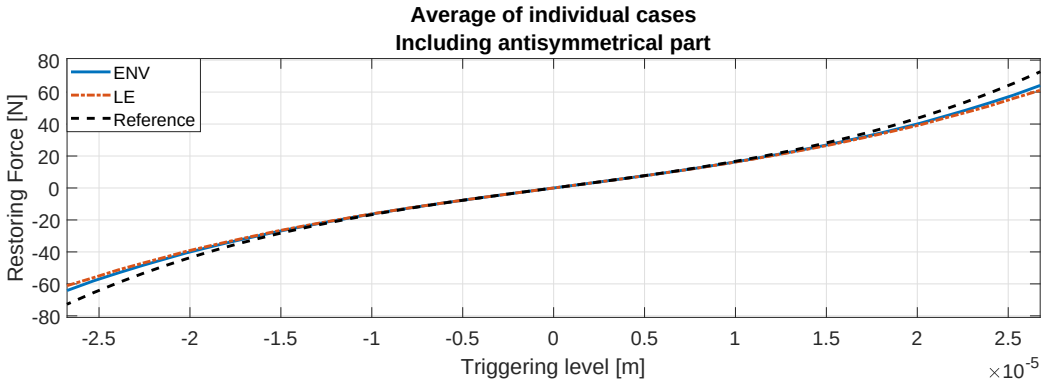

Figure 7: The estimated restoring forces are compared to a reference, calculated by Equation (15). The investigated system, is number 10

The evaluation of the accuracy is done by fitting the restoring force to a function in the form

$$F_{rest} = k_3 x^3 + kx \tag{15}$$

and calculating the error of the coefficients, in relation to the system parameters as given in Table 1. The fitting errors for systems with a nonlinearity are presented in Figure 8. The linear coefficient in the restoring force k, is identified very well, below 2.5 % error for all systems. For both LE and ENV, there is a negative bias of approximately -39 % and -28 % respectively, in the identification of the cubic coefficient in the restoring force k_3. What is really interesting here is that the bias is the same, regardless of system parameters.

For the purely linear systems 1, 5, and 9, the linear stiffness coefficient k is determined within ± 0.1 %, with all triggering conditions investigated here, PP, LC, LE, ENV.

Due to the bias being the same for systems with a nonlinearity, a correction factor β is introduced in the calculation of the restoring force

$$F^{\dagger}_{rest}(Tl_i) = k^*(Tl_i) \cdot \frac{Tl_i}{\beta}. \tag{16}$$

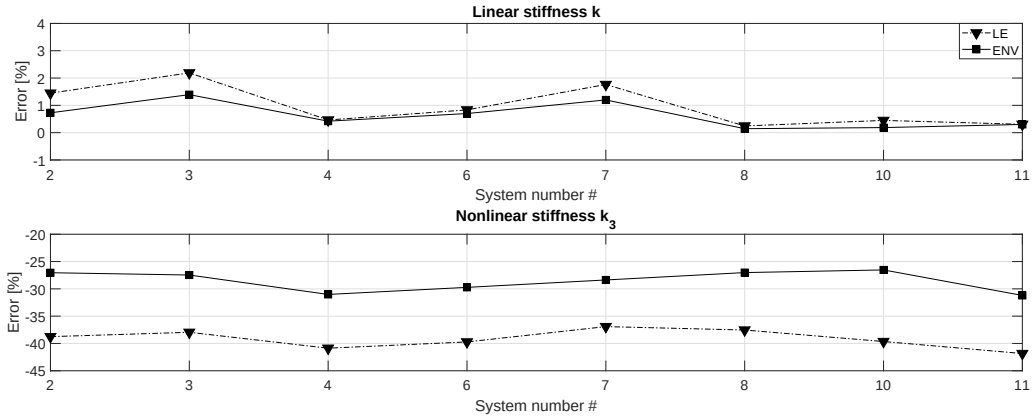

Figure 8: Error in fitted stiffness coefficients for both linear and nonlinear terms, plotted against system number

The displacement term is now proportional to the triggering level. Interpreting the restoring force now, leads to the modal parameters being extracted at the triggering level, but the system parameters are extracted at a response level proportional to the triggering level.

The correction factor is found empirically for the triggering conditions, to be $\beta_{LE} = 1.28$ and $\beta_{ENV} = 1.19$. The restoring force, for both LE and ENV, calculated with the corrected displacement term, is compared in Figure 9, where the reference force is calculated by inserting the stiffness coefficients and the corrected displacement term in Equation (15). β corrected the estimated restoring force to fit with the reference very effectively, as can be seen in Figure 10, where the fitting errors for the cubic coefficient is presented. The error is within $\pm 5\%$ for all nonlinear systems, which is considered an excellent result. The estimation of the linear term remains unchanged with the correction factor.

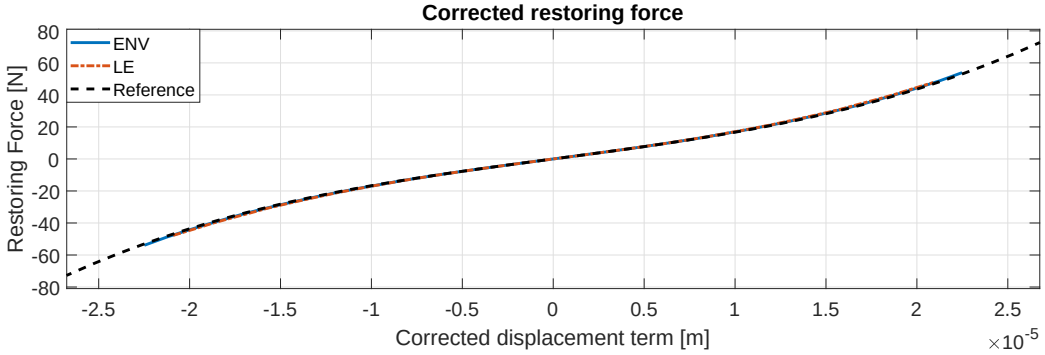

Figure 9: Estimated restoring forces, calculated with the corrected displacement term $\frac{Tl_i}{\beta}$ using Equation (16), compared to a reference calculated with Equation (15). The investigated system, is number 10

It is also investigated how good the fitting of the restoring forces is, calculated from only one case. System 8 is excited by a force with rms level of 33.5 N, and there are 16 triggering levels in the interval $[\sigma_y, 2.5\sigma_y]$, ultimately resulting in 16 points on the curve representing the restoring force as a function of the corrected displacement term. The fitting is a success and the errors for the linear term k, are 0.8 % and 0.1 % for LE and ENV respectively, the errors for the cubic term k_3 is -14.5 % and 0.4 % for LE and ENV, respectively. This means that a single case, where the excitation force is large enough to excite the system beyond the linear regime, is enough to identify the nonlinearity quite well.

The exact nature of β is not well understood at this point, and the present study shows only a dependence of triggering condition. The need for a correction factor stems from the triggering level being a poor substitute for $x(t)$ in Equation (2). The triggering level is a fixed number, while $x(t)$ is a random process, and in

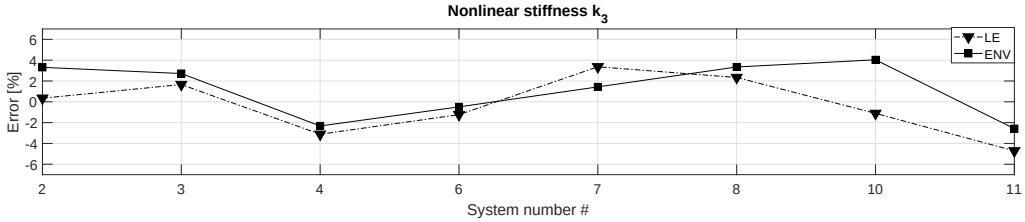

Figure 10: Fitting error for the cubic coefficient in the corrected restoring force

Equation (2), these will cause different outcomes, due to its nonlinearity. In the present study, the excitation force $F(t)$ is normally distributed, and it is expected that a different β will be found for other statistical distributions.

During the investigations, it was discovered that the parameter identification methods had greater difficulty finding stable poles in the stabilization diagrams when the nonlinear systems were excited by a greater force. This phenomenon is illustrated in Figure 11, where system 4 is excited by a medium force level, and a high force level. The RD signatures illustrated are with the same triggering level, and are the 100 lags used in the parameter estimation, the two are almost indistinguishable. The parameter estimation method is Prony, and the difference between the stabilization diagrams is clear. The top one, for the medium force level, has a very clear column of stable pole, represented by green $+$-symbols around 10 Hz. Note how, once the poles are stable, they stay stable as the model order increases, as is expected. For the high force level, the column is now a mix of stable and unstable poles. This is not usual behavior, and is attributed to the nonlinearity, but the exact cause is unknown. This phenomenon is consistent to a varying degree for all systems and parameter estimation methods tested.

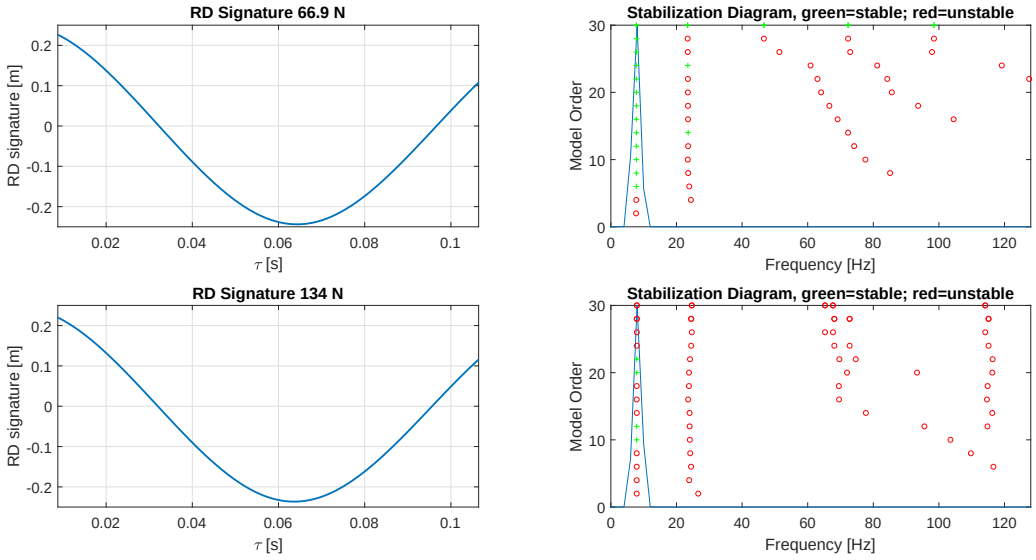

Figure 11: Application of Prony on RD signature found with LE of system 4 with a triggering level of 0.2658 m. The top row shows a medium force excitation, and the bottom row shows a high force excitation

5 Conclusions

The presence of a nonlinearity in the restoring force can be detected in a single response time history, by applying the RD technique at multiple triggering levels, and inspecting the RD signatures to see that properties,

in addition to the scaling, are changing with the triggering level. Of the four RD technique triggering conditions investigated in the present study, PP and LC have been found unable to linearize the modal parameters of the Duffing oscillator independently of the excitation force. The frequency is increasingly overestimated and the damping estimates becomes completely unreliable, when an increasing force excites the system. LE and ENV can successfully linearize the modal parameters, and, when introducing the correction factor β, identify the nonlinear system parameter k_3 with ± 5 % accuracy. The linear stiffness parameter k has been identified with approximately ± 2 % accuracy regardless if the restoring force is linear or nonlinear. For low excitation levels, the damping is accurately estimated using LE and ENV. When the level of excitation force gets large enough, there is a positive bias in the damping estimation method, while the true relative damping is decreasing. These two factors leads to high errors in damping estimates for high levels of excitation force.

Acknowledgements

The authors acknowledge the funding received from Centre for Oil and Gas - DTU/Danish Hydrocarbon Research and Technology Centre (DHRTC).

References

[1] H. A. Cole *On-the-line Analysis of Random Vibrations* AIAA/ASME 9th Structural Dynamics Materials Conference (1968)

[2] S. R. Ibrahim, K. R. Wentz, J. Lee *Damping Identification From Non-Linear Random Responses Using a Multi-Triggering Random Decrement Technique* Mechanical Systems and Signal Processing (1987)

[3] A. P. Jeary *Establishing non-linear damping characteristics of structures from non-stationary response time-histories* The Structural Engineer, Volume 70 (1992)

[4] Y. Tamura, S. Suganuma *Evaluation of amplitude-dependent damping and natural frequency of buildings during strong winds* Journal of Wind Engineering and Industrial Aerodynamics (1996)

[5] Z. Huang, M. Gu *Envelope Random Decrement Technique for Identification of Nonlinear Damping of Tall Buildings* Journal of Structural Engineering, Volume 142 issue 11 (2016)

[6] T. Reynolds *Amplitude Dependence of Modal Properties in Lateral Vibration of Timber Buildings* Proceedings of 24th International Congress on Sound and Vibration (2017)

[7] S. S. Rao *Mechanical Vibrations* Prentice Hall Upper Saddle River (2011)

[8] A. Brandt *Noise and vibration analysis: signal analysis and experimental procedures* John Wiley & Sons (2011)

[9] J. C. Asmussen *Modal Analysis Based on the Random Decrement Technique*, University of Aalborg, Department Building Technology and Structural Engineering, Denmark (1997).

[10] R. Brincker, C. Ventura *Introduction to Operational Modal Analysis* John Wiley & Sons (2015)

[11] J. S. Bendat, A. G. Piersol *Random data: analysis and measurement procedures* John Wiley & Sons (2011)

[12] K. Ahlin, M. Magnevall, A. Josefsson *Simulation of force response in linear and nonlinear mechanical systems using digital filters*, International Conference on Noise and Vibration Engineering (2006)

[13] R. Prony *Essai Expérimental et analytique: sur les lois de la dilatabilité de fluides élastique et sur celles de la Force expansive de la vapeur de l'eau et de la vapeur de l'alkool, à différentes températures.*, Journal de l'École Polytechnique Floréal et Plairial (1795)

[14] Allemang, Randall J. and Brown, David L. *Experimental Modal Analysis and Dynamic Component Synthesis. Volume 3. Modal Parameter Estimation* University of Cincinnati, Department of Mechanical and Industrial Engineering (1987)

[15] S. R. Ibraham, E. C. Mikulcik *A method for the direct identification of vibration parameter from the free responses* Shock and Vibration Bulletin (1977)

[16] A. Brandt *ABRAVIBE - A MATLAB toolbox for noise and vibration analysis and teaching* University of Southern Demark, Department of Technology and Innovation (2018)